Systems/Circuits

Beta Oscillation Dynamics in Extrastriate Cortex after Removal of Primary Visual Cortex

 Joscha T. Schmiedt,[1] Alexander Maier,[2] Pascal Fries,[1,3] Richard C. Saunders,[4] David A. Leopold,[4,5] and Michael C. Schmid[1]

[1]Ernst Strüngmann Institute (ESI) for Neuroscience in Cooperation with Max Planck Society, 60528 Frankfurt, Germany, [2]Vanderbilt University, Department of Psychology, Nashville, Tennessee 37240, [3]Donders Institute for Brain, Cognition and Behaviour, Radboud University, 6525 EN Nijmegen, The Netherlands, [4]Laboratory of Neuropsychology, National Institute of Mental Health, Bethesda, Maryland 20892, and [5]Neurophysiology Imaging Facility, National Institute of Mental Health, National Institute of Neurological Disorders and Stroke, and National Eye Institute, Bethesda, Maryland 20892

The local field potential (LFP) in visual cortex is typically characterized by the following spectral pattern: before the onset of a visual stimulus, low-frequency oscillations (beta, 12–20 Hz) dominate, whereas during the presentation of a stimulus these oscillations diminish and are replaced by fluctuations at higher frequencies (gamma, >30 Hz). The origin of beta oscillations *in vivo* remains unclear, as is the basis of their suppression during visual stimulation. Here we investigate the contribution of ascending input from primary visual cortex (V1) to beta oscillation dynamics in extrastriate visual area V4 of behaving monkeys. We recorded LFP activity in V4 before and after resecting a portion of V1. After the surgery, the visually induced gamma LFP activity in the lesion projection zone of V4 was markedly reduced, consistent with previously reported spiking responses (Schmid et al., 2013). In the beta LFP range, the lesion had minimal effect on the normal pattern of spontaneous oscillations. However, the lesion led to a surprising and permanent reversal of the normal beta suppression during visual stimulation, with visual stimuli eliciting beta magnitude increases up to 50%, particularly in response to moving stimuli. This reversed beta activity pattern was specific to stimulus locations affected by the V1 lesion. Our results shed light on the mechanisms of beta activity in extrastriate visual cortex: The preserved spontaneous oscillations point to a generation mechanism independent of the geniculostriate pathway, whereas the positive beta responses support the contribution of visual information to V4 via direct thalamo-extrastriate projections.

Key words: blindsight; cortex; monkey; neurophysiology; oscillation; V4

Introduction

Neuronal oscillations often appear in both mesoscopic and macroscopic electric field measurements. They are thought to largely reflect synchronous subthreshold synaptic activity generated by local or remote input into an area (Buzsáki et al., 2012) and are an ubiquitous feature of sensory and motor systems (Buzsáki, 2006). The frequencies of these rhythmic phenomena tend to vary in a state-dependent manner, ranging from slow/delta rhythms (0.5–4 Hz) during sleep (Crunelli and Hughes, 2010) to high-frequency oscillations in the gamma frequency range during states of active stimulus processing (Fries, 2009). The intermediate beta frequency range (12–20 Hz) has seen increased interest in

recent years as these rhythms are frequently observed in both sensorimotor (Kilavik et al., 2013) and visual cortex (Engel and Fries, 2010) but have not been conclusively attributed to specific functions. In mammalian visual cortex, beta range fluctuations in the local field potential (LFP) are prominent during the deployment of top-down attention (Lopes da Silva et al., 1970a; Bekisz and Wróbel, 2003; Buschman and Miller, 2007; Bosman et al., 2012; Grothe et al., 2012), working memory allocation (Tallon-Baudry et al., 2004; Salazar et al., 2012), subjective stimulus visibility (Wilke et al., 2006; Maier et al., 2008), and other tasks aimed at probing cognitive processes (Engel and Fries, 2010).

The precise mechanism underlying the generation of beta oscillations in visual cortex is not well understood; in particular, it remains unknown how beta rhythms are shaped by local and/or remote neural sources. It has been suggested that bottom-up (i.e., stimulus-driven) input to an area causes a reduction in oscillatory activity in the beta frequency range, whereas top-down (i.e., endogenously generated) input leads to an enhancement (Engel and Fries, 2010). By combining selective lesions of primary visual cortex (V1) with longitudinal recordings in higher-order visual area 4 (V4) of behaving macaque monkeys, we directly address here the influence of cortical V1 feedforward input on the formation of beta oscillations in the LFP of area V4. Whereas V4 spiking (Schmid et al., 2013) and gamma range activity show a strong reduction following V1 lesions, beta oscillations follow a surpris-

ingly different pattern. Removing the major feedforward sensory input to V4 (Barone et al., 2000) did not eliminate spontaneously occurring beta oscillations. Instead, visual stimulation of V4 in the absence of V1 input led to an enhancement of beta oscillations that was sensitive to the particular parameters of the stimulus. We will discuss this finding and its implications for the generation and possible functional roles of beta oscillations in the context of feedforward and feedback signals along the visual pathway.

Materials and Methods

Subjects. Two healthy adult female rhesus monkeys (*Macaca mulatta*, Monkey B and Monkey F) with prior V1 lesions in the right hemisphere were used in the study. All procedures were in accordance with the Institute for Laboratory Animal Research Guide for the Care and Use of Laboratory Animals and approved by the Animal Care and Use Committee of the National Institute of Mental Health.

Surgical procedures. As described by Schmid et al. (2013), briefly, a chronic "Utah" array of 1.5-mm-long microelectrodes (Blackrock Microsystems) was implanted on the prelunate gyrus in visual area V4. Two weeks later, following the first period of recordings, the part of V1 corresponding to horizontal meridian was lesioned by aspiration while the representation of the vertical meridian was left intact.

Behavioral task and visual stimulation. Visuomotor capacities before and after the V1 lesion (see Fig. 1E) were assessed with a detection task. After a fixation period of 1 s, a 0.2° diameter dot of one of four contrast levels could appear either on the vertical meridian (3.5°–4° eccentricity), on the horizontal meridian (3.5°–5.3° eccentricity), or no stimulus appeared (catch trial). Animals were rewarded if they performed a single saccade to the appearing dot or kept fixating during catch trials.

Visual stimulation with parallel electrical recording was performed in a passive fixation task as described by Schmid et al. (2013). Briefly, monkeys were trained to maintain fixation for at least 2 s within maximally 1° radius of a centrally presented fixation spot while various visual stimuli were displayed on the screen. Animals were rewarded after the presentation of 3 or 4 stimuli. Stimuli were presented for 500 ms and consisted of square-wave gratings with a diameter of 1° or 1.5°, displayed at either one of the following positions: (0°, −3.5°); (3°, −3°); (3.5°, 0°), of which in this study the first position near the vertical meridian was used as control and the last position near the horizontal meridian within the lesion-affected part of the visual field ("lesion stimulus"). The gratings were either static or slowly drifting at 0.3°/s or 0.5°/s and varied with respect to spatial frequency (0.7°/s–10°/s), direction (0°, 90°, 180°, 270° with two being equal for static gratings) and luminance contrast (low vs high, only high contrast considered here). Typical numbers of stimulus presentations per session were between 1000 and 1300. The data presented here comprise periods during which the monkeys had V1 intact and were fully acquainted with the detection task (Monkey F: 5 sessions from 10 to 1 d before the lesion, Monkey B: 7 sessions from 15 to 1 d before the lesion) and a period of several weeks after the V1 lesion surgery when visual detection was reestablished (13 sessions from 30 to 72 d after the lesion, 5 sessions from 40 to 53 d after the lesion).

Neurophysiological recordings. All electrophysiological recording sessions were carried out in an electromagnetically shielded cabin. Voltages were measured against a reference wire located subdurally over parietal cortex. The impedance of the recording electrodes ranged between 150 kΩ and 1 MΩ at 1 kHz. Extracellular voltages were amplified, filtered between 0.1 Hz and 12 kHz, and digitized at 24,414.1 Hz using a 64 channel RZ2 recording system (Tucker Davis Technologies). Electrodes were selected for data analysis if at least three recording sessions before and after the V1 lesion showed a noise and artifact-free signal.

Data analysis. All data were analyzed with the MATLAB (R2011a, MathWorks) toolbox FieldTrip (Oostenveld et al., 2011) (http://fieldtrip.fcdonders.nl) and custom-written routines. LFPs were extracted from raw signals by downsampling to 1017.25 Hz. LFP wavelet time-frequency analysis was performed with a Morlet wavelet of 7 cycles length (Field-Trip parameter "width," corresponding to a spectral bandwidth of 2.14 Hz at 15 Hz) at 89 logarithmically spaced frequencies between 7.6 and
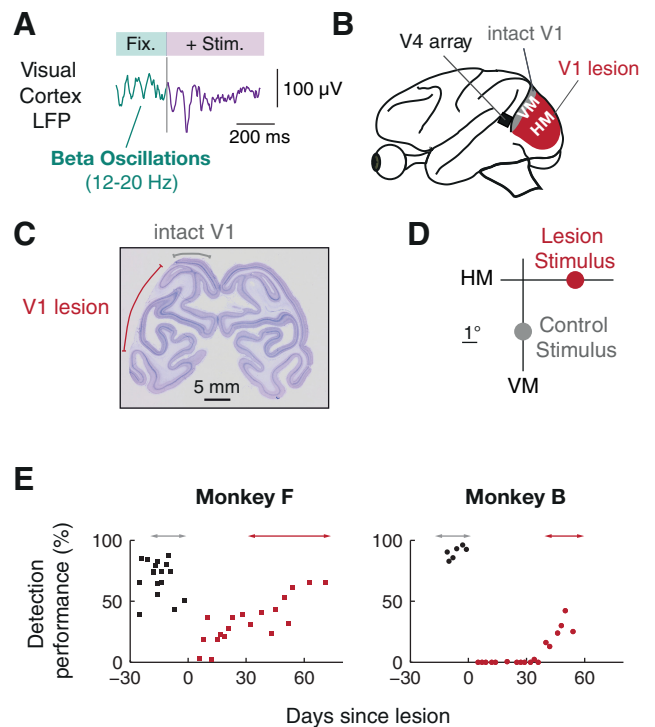
Figure 1. Longitudinal investigation of beta rhythms (12–20 Hz) in the LFP of area V4 with and without V1 input by selective ablation of V1. *A*, During task periods without transient sensory input, such as active fixation (Fix.) before the onset of a stimulus (Stim.), the LFP in visual cortex of behaving subjects is often dominated by rhythmic fluctuations in the beta frequency range (12–20 Hz). *B*, To investigate the role of bottom-up input for the generation of these beta oscillations, we recorded from midlevel area V4 with chronically implanted arrays before and after a targeted aspiration lesion in V1. The lesion was placed to eliminate the V1 representation of the horizontal meridian (HM) between ∼2–7° of visual eccentricities (red) while leaving the lower vertical meridian (VM) representation, close to lunate sulcus, intact (gray). *C*, Example coronal section of V1 showing extent of lesioned (red line) and intact (gray line) tissue for Monkey B. Note the loss of gray matter in the targeted area. *D*, Stimulus locations throughout the paper are labeled lesion stimulus (LS) for stimuli inside the lesion-affected visual space around the HM and control stimulus (CS) for stimuli outside, close to the VM. *E*, Behavioral performance in a detection task before and after V1 lesion with dot stimuli around the lesion stimulus location. Arrows indicate time period of LFP recordings.

400 Hz. Stimulus-induced power changes were quantified as percentage change from the 250 ms baseline power averaged across trials. Power in a time-frequency window was determined by averaging across time and frequency. The latency of the stimulus-induced beta power changes were determined as the first time point reaching 90% of the peak value in the session-averaged beta power time course. For all prelesion and control stimulus data, the peak was defined as the minimum value in the 50–400 ms window after stimulus onset. For the lesion stimulus after lesion, the peak was defined as the maximum power value in the same time window.

Results

The goal of our experiments was to directly test the effect of permanent V1 lesions on the spectral properties of visual responses in area V4 (Fig. 1A) of macaque extrastriate cortex. Detailed retinotopic assessment of V1 and V4 by fMRI guided the planning of our surgical procedures (Schmid et al., 2013). We first implanted multielectrode arrays into the dorsal part of area V4 at a position responsive to parafoveal visual stimulation in the lower right quadrant of the visual field. After recovery from the implantation, over the course of 2 weeks, we obtained LFP recordings during visual task performance, as a baseline with intact V1. Subsequently, we surgically removed V1 gray matter straddling the horizontal meridian representation (Fig. 1B). Care was

taken to spare a section of the cortex ~5 mm in width along the lunate sulcus (which corresponds to the visual representation of the visual vertical meridian and the boundary to area V2). Using this selective lesioning approach, our study contrasted V4 LFP responses to visual stimuli with V1 input intact versus V1 removed, regardless of the time point of assessment (Fig. 1C,D). Postmortem histological assessment of the occipital lobes of both monkeys confirmed the complete loss of gray matter in the targeted area of V1 as well as the preservation of striate cortex in the control region (Fig. 1C).

To assess the impact of the V1 lesion on the monkeys' visuomotor capacities, we tested the monkeys on a simple task in which they had to detect and saccade toward a small patch of light. While both monkeys achieved very good performance under V1 intact conditions, lesioning V1 had a detrimental effect on performance, that is, the monkeys were unable to detect stimuli presented at the horizontal meridian (lesion stimulus) (Fig. 1E). However, following a recovery period of 30–40 d with daily testing on the detection task, both monkeys had partially recovered their detection capabilities and reached performance values ranging from 23%–66% in Monkey F and 13%–42% in Monkey B.

For the electrophysiological assessment, we focused our analysis on the time periods before and >30 d after the surgical intervention (i.e., when the monkeys had regained some of their visuomotor capacities; Monkey F: 30–72 d after lesion; Monkey B: 40–53 d after lesion). The basic testing procedure across all experimental conditions entailed passive fixation on a centrally presented spot, while stimuli were shown on a screen. After 250 ms of fixation, a drifting or static square-wave grating stimulus (high contrast, varying drift direction, and spatial frequency, 70–90 presentations per session) was presented in parafoveal regions to elicit visually triggered LFP responses while the monkey continued to fixate. Stimuli were either placed in the lesion-affected part of visual space, that is, the horizontal meridian (lesion stimulus), or on the vertical meridian (control stimulus). During the times when testing was performed under V1 intact conditions, the prestimulus LFP was often dominated by voltage fluctuations in the beta frequency range (12–20 Hz; Fig. 2A,D, left). Following stimulus onset and a brief broadband response, these low-frequency fluctuations decreased in amplitude, and a mixture of broadband and oscillatory high-frequency gamma activity (>50 Hz) instead dominated the LFP (for an example, see Fig. 3A). The resulting spectral change of the LFP was evident as a decrease in the baseline-normalized beta power and an increase in gamma band power. This effect of visual stimulation causing a shift from high-amplitude, low-frequency activity toward low-amplitude, high-frequency activity has been observed in a large number of studies on visual cortical responses (Gray and Singer, 1989; Taylor et al., 2005; Ray and Maunsell, 2011).

Prestimulus beta rhythms in V4 are still present after V1 lesion

Following the V1 lesion and subsequent partial behavioral recovery (Monkey F: 30–72 d after lesion; Monkey B: 40–53 d after lesion) beta oscillations during the prestimulus period (Fig. 2) were prominent in the raw LFP (Fig. 2A,D, right) and manifested as peaks in the power spectra ~15 and 14 Hz in Monkey F and Monkey B, respectively (Fig. 2B,E). The mean amplitude of the oscillation was unchanged in Monkey F (Fig. 2A–C, p > 0.05, n = 47 electrodes averaged across 5 sessions prelesion and 11–13 sessions after lesion, Wilcoxon signed rank test) and enhanced by 23 ± 4.4% in Monkey B (Fig. 2D–F, p < 10^{-5}, n = 53 electrodes averaged across 7 sessions prelesion and 3–5 sessions after lesion).

Prestimulus period
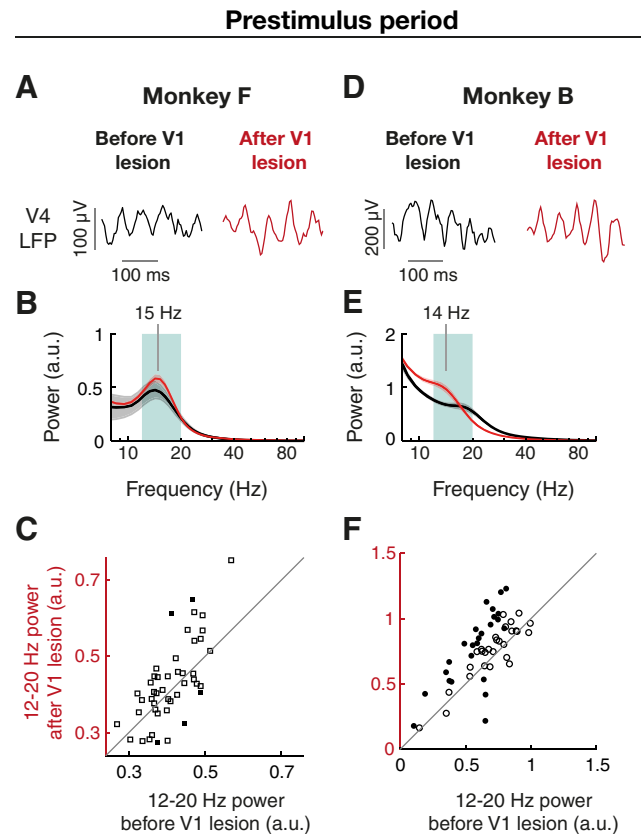
Figure 2. Beta oscillations during active fixation in area V4 are preserved after selective removal of V1. **A**, Example prestimulus beta oscillations of the unfiltered V4 LFP before (black, left) and after V1 lesion (red, right). **B**, Absolute power spectrum of the prestimulus period before (black, n = 5 sessions, each comprising 1000–1300 trials) and after (red, n = 13 sessions) from an example V4 electrode in Monkey F, averaged across trials and sessions. Gray and red shadings represent SEM across sessions before and after lesion, respectively. **C**, Distribution of power in the beta frequency range (12–20 Hz, green shading in **B**) during prestimulus period before and after V1 lesion. Each dot represents the beta-band power at a recording site averaged across sessions. Filled and open symbols represent recording sites with significant or nonsignificant changes in power (p < 0.05, independent samples t test), respectively. Gray line indicates identical prelesion and postlesion power. **D–F**, Example beta oscillations (**D**), wavelet spectrum (**E**), and beta power distribution (**F**) for Monkey B before (n = 7 sessions) and after (n = 5 sessions) V1 lesion.

On the individual electrode level, in Monkey F only a small fraction showed significant changes in beta power, with a decrease in 2 (4%) electrodes and increase in other 2 (4%) electrodes (independent samples t test, p < 0.05, electrodes and sessions as before). In Monkey B, 21 (40%) electrodes showed a significant increase and 3 (6%) electrodes a decrease in beta power. These findings demonstrate that the generation of V4 beta oscillations is not dependent on input from V1.

Differential effects of V1 lesion on V4 beta and gamma dynamics

Under normal conditions, the presentation of a visual stimulus leads to a reduction in the amplitude of beta LFP oscillations (Fig. 3A). Following the lesion, however, there was a notable reversal of this effect: visual stimulation with a slowly drifting grating in the lesion-affected visual space now led to a beta power enhancement (Fig. 3B). This postlesion stimulus-induced beta power enhancement was significantly different from zero in both monkeys (p < 10^{-6}, Wilcoxon signed rank test, n = 47 and 53 electrodes in Monkey F and Monkey B, respectively). Compared with the pre-
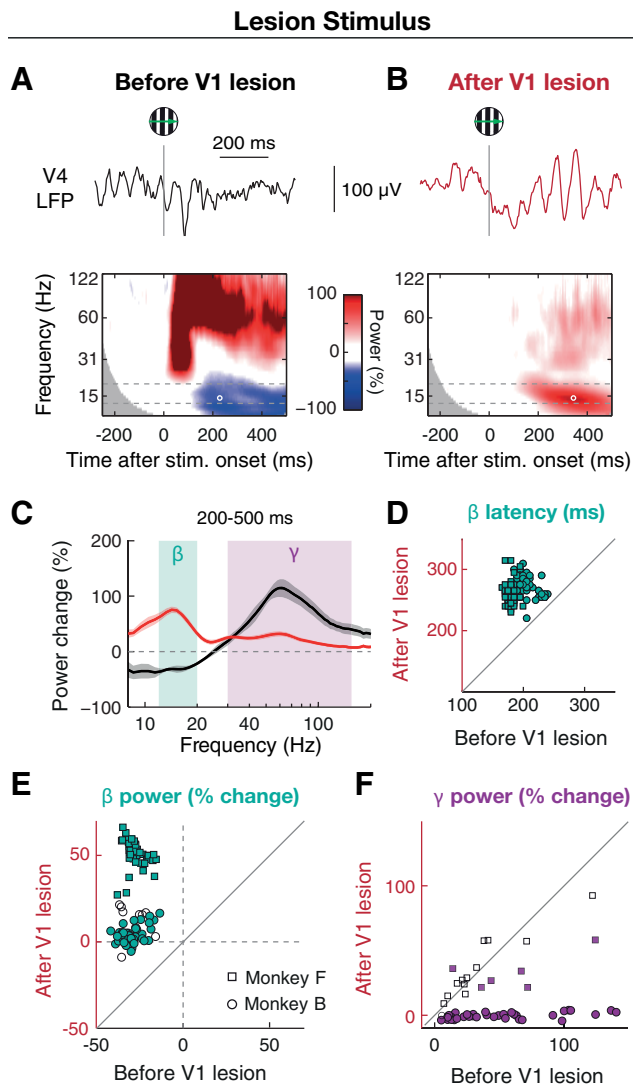
Lesion Stimulus

Figure 3. Visual stimulation in lesion-affected visual space induces strong beta (12–20 Hz) oscillations in V4 instead of decreasing beta power. ***A***, Example LFP responses to a moving grating stimulus (high contrast, varying spatial frequency, and drift direction) in the lesion-affected part of visual space from a recording site in Monkey F before the V1 lesion. Upper row, Single trial LFP trace. Gray line indicates stimulus onset. Lower row, Session-averaged ($n = 5$), baseline-normalized wavelet power spectra from an example electrode in Monkey F (data as in Fig. 2). White circle represents peak latency within the beta frequency band (dashed lines). ***B***, Same as ***A*** for data from after the V1 lesion ($n = 11$ sessions). Note the unusual stimulus-induced beta oscillations visible in both single trials and average. ***C***, Baseline-normalized power spectra from example recording site in ***A*** averaged across 200–500 ms period and sessions for lesion stimulus, before (black) and after (red) V1 lesion. Shadings surrounding curves represent SEM across sessions. ***D***, Distribution of beta power peak latency before and after V1 lesion. ***E***, Distribution of baseline-normalized power in beta band before and after V1 lesion for lesion stimulus. Each dot represents a power value from one recording site averaged across the beta band, 200–500 ms period, and sessions. ***F***, Same as ***E*** for the gamma frequency band (30–150 Hz). ***E***, ***F***, Open and filled symbols represent recording sites with nonsignificant and significant changes in power on the individual electrode level ($p < 0.05$, independent samples t test), respectively.

lesion condition, the baseline-normalized beta power in the 200–500 ms and 12–20 Hz time-frequency window increased from $-27.1 \pm 0.84\%$ to $51 \pm 1.1\%$ in Monkey F ($p < 10^{-8}$, $n = 47$ electrodes, Wilcoxon signed rank test) and from $-29 \pm 0.9\%$ to $5 \pm 0.9\%$ in Monkey B ($p < 10^{-9}$, $n = 53$ electrodes) (Fig. 3C). On the individual electrode level, 47 of 47 (100%) and 43 of 53 (81%) electrodes showed a significant increase in stimulus-induced

beta power (independent samples t test, $p < 0.05$, sessions as above) (Fig. 3E). Thus, lack of V1 input appeared to unmask the stimulus-induced modulation of beta oscillations.

To obtain more information with respect to mechanistic changes that may have contributed to this effect, we compared the latencies of the stimulus-induced beta modulation before and after the V1 lesion. The beta power enhancement observed under V1 lesion conditions reached its peak at 260 ± 2.8 ms and 274 ± 2.3 ms after stimulus onset (Fig. 3D; see 5A) for Monkey F and Monkey B, respectively. In comparison, the stimulus induced beta power decrease under V1 intact conditions had a latency of 179 ± 1.0 ms and 207 ± 2.1 ms in Monkey F and Monkey B, respectively. This means that the postlesion positive beta peak occurred by $\sim 65–85$ ms significantly later than the negative peak before the lesion ($p < 10^{-9}$ in both monkeys, Wilcoxon signed rank test).

In addition to the changes in the beta oscillation dynamics, we also examined the effects of the V1 lesion on faster LFP oscillatory activity (i.e., in the gamma range, which is thought to be strongly dependent on feedforward input) (Bosman et al., 2012). In contrast to the general increase in the stimulus-induced beta power, effects on the stimulus-induced gamma power (30–150 Hz, late time window 200–500 ms, same sessions and trials as for beta) were more spatially confined. In sites that were well activated by the stimulus before the lesion (power increase from baseline >25%, $p < 0.05$, independent samples t test), gamma power was reduced after the V1 lesion (Fig. 3C,F). In Monkey B, stimulus-elicited gamma power was drastically decreased from $70 \pm 7.3\%$ prelesion to $0.3 \pm 0.4\%$ postlesion ($n = 23$ electrodes, Wilcoxon signed rank test, $p < 10^{-7}$, sessions as above), which was significant in 23 of 23 (100%) individual recording sites (independent samples t test, $p < 0.05$). In Monkey F, this gamma decrease was less pronounced, from $64 \pm 11\%$ prelesion to $44 \pm 6\%$ postlesion ($p = 0.037$, Wilcoxon signed rank test, $n = 10$ electrodes) with 4 of 10 electrodes showing significant decreases ($p < 0.05$, independent samples t test).

Reversal of beta oscillation dynamics is restricted to lesion-affected visual space

Importantly, the lesion-induced reversal of beta dynamics was specific to stimuli that were presented in the lesion-affected visual space and was not seen for the identical control stimuli that invoked visual processing in V1 as they were presented outside the lesion zone (Fig. 1D). Stimulation at the vertical meridian resulted in a decrease in low frequency and an increase in high-frequency power (Fig. 4). In contrast to the stimulus in the lesion-affected space, beta power values for the control stimulation (Fig. 4E) were either further decreased from the prelesion baseline in Monkey F, from $-21.9 \pm 0.83\%$ to $-45 \pm 1.2\%$ ($p < 10^{-8}$, Wilcoxon signed rank test, $n = 47$ electrodes) or minimally increased in Monkey B with $-34 \pm 1.2\%$ before and $-32 \pm 1.1\%$ after the lesion ($p = 0.025$, Wilcoxon signed rank test, $n = 53$ electrodes). On the individual electrode level, in Monkey F 44 of 47 (94%) electrodes showed a significant decrease of stimulus-induced beta power, whereas in Monkey B 8 of 53 (15%) showed a significant increase and 1 of 53 (2%) a significant decrease (independent samples t test, sessions as before). The gamma frequency range was also affected with an increase from $40 \pm 3.6\%$ to $74 \pm 8.9\%$ in Monkey F ($p = 0.016$, $n = 7$ electrodes, Wilcoxon signed rank test; significant change in 5 (71%) electrodes, independent samples t test) and a decrease in Monkey B from $75 \pm 9.4\%$ to $58 \pm 8.0\%$ ($p = 0.008$, $n = 13$ electrodes; significant change in 2 (15%) electrodes).
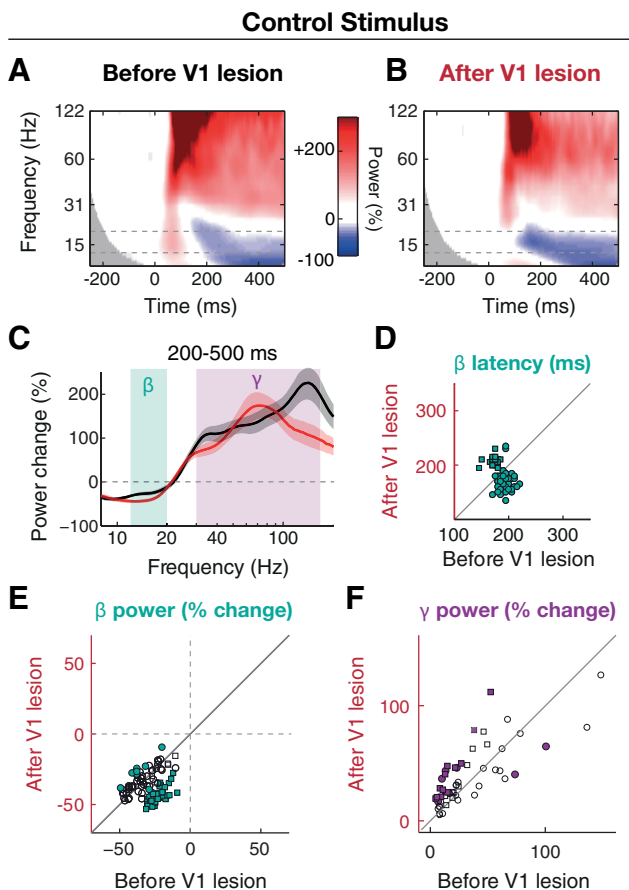
Figure 4. Reversal of stimulus-induced beta oscillation dynamics is restricted to visual stimulation in lesion-affected space. *A*, *B*, Session-averaged, baseline-normalized wavelet power spectra from an example electrode in Monkey B around visual stimulation with drifting grating stimulus (high contrast, varying spatial frequency, and drift correction) at the control stimulus location before (*A*, n = 7 sessions) and after (*B*, n = 4 sessions) the V1 lesion. *C*, Baseline-normalized power spectra from example recording site in *A*, *B* averaged across 200–500 ms period and sessions for lesion stimulus, before (black) and after (red) V1 lesion. Shadings surrounding curves represent SEM across sessions. *D*, Distribution of beta power peak latency before and after V1 lesion *E*, Distribution of baseline-normalized power in beta band before and after V1 lesion for lesion stimulus. Each dot represents a power value from one recording site averaged across the beta band, 200–500 ms period, and sessions. *F*, Same as *E* for the gamma frequency band (30–150 Hz). *E*, *F*, Open and filled symbols represent recording sites with nonsignificant and significant changes in power on the individual electrode level (p < 0.05, independent samples t test), respectively.

Stimulus-induced beta oscillations reflect stimulus content

We previously observed residual, V1-independent spiking activity in V4 that was unusually sensitive to stimulus motion (Schmid et al., 2013). In an effort to assess whether beta oscillations similarly reflected feature-dependent processing of the stimulus, we compared their magnitude following the presentation of static versus slowly drifting gratings (Fig. 5). In both monkeys, the stimulus-driven beta power increase in V4 was significantly stronger for moving than for static stimuli ($p < 10^{-8}$ for both monkeys, Wilcoxon signed rank test), indicating that the observed responses showed some level of stimulus specificity.

Discussion

Our results demonstrate that beta-band oscillations in area V4 are preserved in the absence of V1 input, indicating that they are not generated by a feedforward drive from V1. Moreover, following the ablation of V1, the stimulus-driven power decrease in the beta frequency band was replaced by stimulus-driven power in-
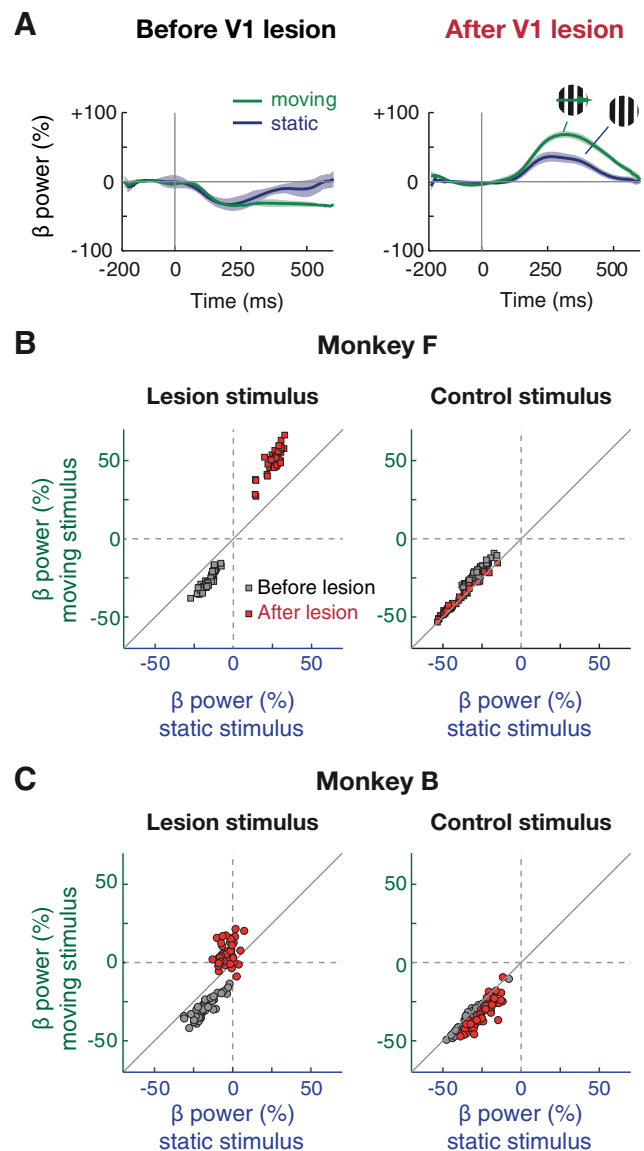
Figure 5. V1-independent beta oscillations are sensitive to motion. *A*, Time course of baseline-normalized power in beta (12–20 Hz) band from example recording site and sessions in Monkey F for moving (green) and static (blue) grating stimuli (high contrast, varying drift direction/orientation, and spatial frequency for both) at the lesion stimulus location. Shading represents SEM. *B*, Distribution of beta power values (200–500 ms) for moving versus static stimuli for lesion (left) and control stimulus (right) from Monkey F (data as in Figs. 3 and 4). *C*, Same as *B* for Monkey B.

crease occurring ~300 ms after stimulus onset. As this effect was limited to the lesion-affected part of visual space, passive volume conduction as a potential contributor to the observed effect can be largely excluded. In addition, stimulus-induced beta power modulation in V1-deafferented V4 was sensitive to stimulus motion, indicating that these changes of the LFP are related to active feature-dependent stimulus processing. In the following, we discuss our findings in the context of what is known about the generation of beta oscillations and their putative contribution to cortical processing.

Beta rhythm in infragranular cortical layers

Beta oscillations in the visual system were described early in the occipital cortex of dogs actively attending a screen (Lopes da Silva et al., 1970a). Yet, compared with other brain rhythms, to date

very little is known about their generation and function in the visual system (Steriade, 1993; Engel and Fries, 2010). On the cellular level, *in vitro* results from rat auditory and somatosensory cortex showed that layer 5 cortical pyramidal neurons can generate beta rhythms (Roopun et al., 2006, 2010). Consistent with this finding are observations from studies showing that alpha to beta band oscillations measured in primate visual cortex are most prominent in the infragranular layers (Sun and Dan, 2009; Buffalo et al., 2011; Maier et al., 2011; Xing et al., 2012). Given an estimated average cortical thickness of ~2 mm and our electrode lengths of 1.5 mm, it is likely that we have primarily sampled beta activity from V4's deep layers. A common observation in studies that assessed oscillatory activity in visual cortex is that the LFP is usually dominated by low-frequency fluctuations before the presentation of salient visual stimuli, which are then reduced during stimulus presentation (Gray and Singer, 1989; Taylor et al., 2005; Fries et al., 2008; Ray and Maunsell, 2011). This effect of stimulus-induced cortical excitation is also evident in our data from area V4 in the V1 intact condition (Figs. 3 and 4). *In vitro* slice studies suggest that an excitatory glutamatergic or cholinergic drive is needed to generate beta oscillations (Roopun et al., 2006, 2010). What might be the source of the V4 beta oscillation and its modulation by visual input?

Beta oscillations may reflect unmasked input from thalamus or neighboring cortex

Our data argue against a contribution of a bottom-up V1 drive contributing to V4 beta oscillations because prestimulus beta power was not affected or, if anything, increased under the lesion condition. Surprisingly, after the lesion, beta power in V4 was no longer diminished following visual input, but instead, beta oscillations were enhanced following the presentation of a stimulus. It is likely that this effect reflects some form of unmasking or plasticity that results from the lack of V1 input and may involve either local or remote circuits. For example, it is conceivable that neurons in layer 4 of V4 release their inhibitory impact on processes in deeper layers when their driving input from V1 is removed. Alternatively, the enhanced beta modulation may indicate the unmasking of alternative input projections. It is likely that at some point these processes invoke the thalamus. The lateral geniculate nucleus (LGN) directly projects to multiple extrastriate areas, including V4 (Fries, 1981; Lysakowski et al., 1988; Rodman et al., 2001; Lyon and Rabideau, 2012), and has been shown to be crucial for V1-independent responses in extrastriate areas (Schmid et al., 2009, 2010). Interestingly, the geniculate input to V4 appears to target primarily the deeper layers (Benevento and Yoshida, 1981) from which we likely recorded and where beta oscillations are most prominent. It is possible that V4 inherits beta oscillatory activity via this projection from LGN as beta oscillations have also been recorded in LGN (Lopes da Silva et al., 1970b, 1970a; Bekisz and Wróbel, 2003; Bastos et al., 2014). This geniculate beta-drive to V4 may get unmasked or even upregulated following the V1 lesion. Other thalamic nuclei are also possible candidate sources for beta rhythmicity in visual cortex, in particular the pulvinar and lateral posterior complex. These higher-order nuclei have been shown to engage in rhythmic activity in the alpha/beta frequency range (Wróbel et al., 2007; Saalmann et al., 2012). The pulvinar, which receives visual input from superior colliculus and projects to visual cortex (Harting et al., 1980; Stepniewska et al., 1999; Adams et al., 2000; Lyon et al., 2010), could trigger a stimulus-related increase in oscillatory activity.

A possible argument against a thalamic origin of V1-independent beta modulations is the relatively long peak latency

of 300 ms after stimulus onset. It is therefore conceivable that the beta oscillations are triggered by input from other cortical areas, including feedback projections, which reach to the infragranular layers of area V4 as well (Barone et al., 2000). The idea of cortical beta oscillations as a spectral signature of top-down feedback signals has gained support from a number of studies that reported beta-band modulation associated with attention (Bekisz and Wróbel, 2003; Buschman and Miller, 2007; Bosman et al., 2012), working memory allocation (Tallon-Baudry et al., 2004; Salazar et al., 2012), or subjective stimulus visibility (Wilke et al., 2006; Maier et al., 2008). In some of these studies, beta oscillations resulted in increased interareal coherence (Buschman and Miller, 2007; Bosman et al., 2012; Salazar et al., 2012) and were most pronounced in cortical layers 5 and 6 (Maier et al., 2008; Sun and Dan, 2009; Buffalo et al., 2010). However, a recent study reported beta oscillations that did not exhibit attentional modulation in area V4 of monkeys with prefrontal cortex lesions (Gregoriou et al., 2014). Therefore, areas other than prefrontal cortex likely contribute to the observed beta oscillation dynamics in our results.

Irrespective of the ultimate neuronal mechanism leading to the formation of beta oscillations, it appears to become unmasked or perhaps even plastically upregulated after lesioning V1. As the changes in beta oscillation dynamics were observed during a time period when visuomotor detection capacities had substantially recovered after the surgery (Mohler and Wurtz, 1977), it is tempting to speculate that the beta increase may reflect or perhaps even directly contribute to the observed behavioral recovery.

Dependence of gamma range activity on feedforward input

In contrast to LFP beta oscillations in visual cortex that are present before the onset of a visual stimulus, oscillatory activity in the gamma frequency band is usually associated with the presence of a visual stimulus (Gray and Singer, 1989; Fries, 2009; Ray and Maunsell, 2011). It was hypothesized that gamma oscillations could be related to or even mediate feedforward processing (Bosman et al., 2012) of visual stimuli. In our data, similar to previous assessment of spiking and fMRI activity in V4 after removal of V1 input (Schmid et al., 2010, 2013), LFP activity in the gamma range in V4 was decreased or abolished following the V1 lesion. Therefore, feedforward input from V1 appears to be necessary for the full emergence of gamma oscillations at the level of V4.

Distinguishing alpha from beta oscillations

The beta oscillations and their modulation by the stimulus that we observed were ~15 Hz in both monkeys (Figs. 2*A*,*E* and 3*C*,*D*). This frequency lies at the lower end of the classical beta 13–30 Hz (Kilavik et al., 2013) frequency band, raising the question whether the generative mechanism of the beta oscillations in our study is distinct from the one for alpha oscillations, which are usually considered to be in the 8–12 Hz range in both humans (Haegens et al., 2014) and monkeys (Bollimunta et al., 2008) as well as other species. One important difference between the two frequency bands in previous studies seemed to be that beta rhythms were enhanced in attentive behavior (Lopes da Silva et al., 1970a; Bekisz and Wróbel, 1993), whereas alpha rhythms were strongest when attention was away from visual stimuli (Lopes da Silva et al., 1980; Bollimunta et al., 2011; Haegens et al., 2014). In our case, the monkeys were attentively fixating on the screen to receive reward and were also trained on other visual tasks that required attention to the visual domain. This makes it conceivable that the rhythm observed in our data is rather asso-

ciated with an activated state. However, based only on frequency range, without more targeted experimental manipulations, it is difficult to delineate whether the underlying mechanism has greater overlap with the alpha-generating or beta-generating networks.

A final conclusion on the origin of the beta rhythm withstanding, our data conclusively demonstrate that the feedforward drive from V1 is not necessary for the initiation and maintenance of V4 rhythmic activity in the beta range. Rather, V1 input seems to be required to break low-frequency rhythms and evoke an activated state (for a similar mechanism in the thalamocortical system, compare Castro-Alamancos, 2004; Poulet et al., 2012).

References

Adams MM, Hof PR, Gattass R, Webster MJ, Ungerleider LG (2000) Visual cortical projections and chemoarchitecture of macaque monkey pulvinar. J Comp Neurol 419:377–393. CrossRef Medline

Barone P, Batardiere A, Knoblauch K, Kennedy H (2000) Laminar distribution of neurons in extrastriate areas projecting to visual areas V1 and V4 correlates with the hierarchical rank and indicates the operation of a distance rule. J Neurosci 20:3263–3281. Medline

Bastos AM, Briggs F, Alitto HJ, Mangun GR, Usrey WM (2014) Simultaneous recordings from the primary visual cortex and lateral geniculate nucleus reveal rhythmic interactions and a cortical source for gamma-band oscillations. J Neurosci 34:7639–7644. CrossRef Medline

Bekisz M, Wróbel A (1993) 20 Hz rhythm of activity in visual system of perceiving cat. Acta Neurobiol Exp (Wars) 53:175–182. Medline

Bekisz M, Wróbel A (2003) Attention-dependent coupling between beta activities recorded in the cat's thalamic and cortical representations of the central visual field. Eur J Neurosci 17:421–426. CrossRef Medline

Benevento LA, Yoshida K (1981) The afferent and efferent organization of the lateral geniculo-prestriate pathways in the macaque monkey. J Comp Neurol 203:455–474. CrossRef Medline

Bollimunta A, Chen Y, Schroeder CE, Ding M (2008) Neuronal mechanisms of cortical alpha oscillations in awake-behaving macaques. J Neurosci 28:9976–9988. CrossRef Medline

Bollimunta A, Mo J, Schroeder CE, Ding M (2011) Neuronal mechanisms and attentional modulation of corticothalamic alpha oscillations. J Neurosci 31:4935–4943. CrossRef Medline

Bosman CA, Schoffelen JM, Brunet N, Oostenveld R, Bastos AM, Womelsdorf T, Rubehn B, Stieglitz T, De Weerd P, Fries P (2012) Attentional stimulus selection through selective synchronization between monkey visual areas. Neuron 75:875–888. CrossRef Medline

Buffalo EA, Fries P, Landman R, Liang H, Desimone R (2010) A backward progression of attentional effects in the ventral stream. Proc Natl Acad Sci U S A 107:361–365. CrossRef Medline

Buffalo EA, Fries P, Landman R, Buschman TJ, Desimone R (2011) Laminar differences in gamma and alpha coherence in the ventral stream. Proc Natl Acad Sci U S A 108:11262–11267. CrossRef Medline

Buschman TJ, Miller EK (2007) Top-down versus bottom-up control of attention in the prefrontal and posterior parietal cortices. Science 315: 1860–1862. CrossRef Medline

Buzsáki G (2006) Rhythms of the brain. Oxford: Oxford UP.

Buzsáki G, Anastassiou CA, Koch C (2012) The origin of extracellular fields and currents: EEG, ECoG, LFP and spikes. Nat Rev Neurosci 13:407–420. CrossRef Medline

Castro-Alamancos MA (2004) Dynamics of sensory thalamocortical synaptic networks during information processing states. Prog Neurobiol 74: 213–247. CrossRef Medline

Crunelli V, Hughes SW (2010) The slow (<1 Hz) rhythms of non-REM sleep: a dialogue between three cardinal oscillators. Nat Neurosci 13:9–17. CrossRef Medline

Engel AK, Fries P (2010) beta-band oscillations: signalling the status quo? Curr Opin Neurobiol 20:156–165. CrossRef Medline

Fries P (2009) Neuronal gamma-band synchronization as a fundamental process in cortical computation. Annu Rev Neurosci 32:209–224. CrossRef Medline

Fries P, Womelsdorf T, Oostenveld R, Desimone R (2008) The effects of visual stimulation and selective visual attention on rhythmic neuronal synchronization in macaque area V4. J Neurosci 28:4823–4835. CrossRef Medline

Fries W (1981) The projection from the lateral geniculate nucleus to the prestriate cortex of the macaque monkey. Proc R Soc Lond B Biol Sci 213:73–86. CrossRef Medline

Gray CM, Singer W (1989) Stimulus-specific neuronal oscillations in orientation columns of cat visual cortex. Proc Natl Acad Sci U S A 86:1698–1702. CrossRef Medline

Gregoriou GG, Rossi AF, Ungerleider LG, Desimone R (2014) Lesions of prefrontal cortex reduce attentional modulation of neuronal responses and synchrony in V4. Nat Neurosci 17:1003–1011. CrossRef Medline

Grothe I, Neitzel SD, Mandon S, Kreiter AK (2012) Switching neuronal inputs by differential modulations of gamma-band phase-coherence. J Neurosci 32:16172–16180. CrossRef Medline

Haegens S, Cousijn H, Wallis G, Harrison PJ, Nobre AC (2014) Inter- and intra-individual variability in alpha peak frequency. Neuroimage 92:46–55. CrossRef Medline

Harting JK, Huerta MF, Frankfurter AJ, Strominger NL, Royce GJ (1980) Ascending pathways from the monkey superior colliculus: an autoradiographic analysis. J Comp Neurol 192:853–882. CrossRef Medline

Kilavik BE, Zaepffel M, Brovelli A, MacKay WA, Riehle A (2013) The ups and downs of beta oscillations in sensorimotor cortex. Exp Neurol 245:15–26. CrossRef Medline

Lopes da Silva FH, van Rotterdam A, Storm van Leeuwen W, Tielen AM (1970a) Dynamic characteristics of visual evoked potentials in the dog: II. beta frequency selectivity in evoked potentials and background activity. Electroencephalogr Clin Neurophysiol 29:260–268. CrossRef Medline

Lopes da Silva FH, van Rotterdam A, Storm van Leeuwen W, Tielen AM (1970b) Dynamic characteristics of visual evoked potentials in the dog: I. Cortical and subcortical potentials evoked by sine wave modulated light. Electroencephalogr Clin Neurophysiol 29:246–259. CrossRef Medline

Lopes da Silva FH, Vos JE, Mooibroek J, Van Rotterdam A (1980) Relative contributions of intracortical and thalamo-cortical processes in the generation of alpha rhythms, revealed by partial coherence analysis. Electroencephalogr Clin Neurophysiol 50:449–456. CrossRef Medline

Lyon DC, Rabideau C (2012) Lack of robust LGN label following transneuronal rabies virus injections into macaque area V4. J Comp Neurol 520: 2500–2511. CrossRef Medline

Lyon DC, Nassi JJ, Callaway EM (2010) A disynaptic relay from superior colliculus to dorsal stream visual cortex in macaque monkey. Neuron 65:270–279. CrossRef Medline

Lysakowski A, Standage GP, Benevento LA (1988) An investigation of collateral projections of the dorsal lateral geniculate nucleus and other subcortical structures to cortical areas V1 and V4 in the macaque monkey: a double label retrograde tracer study. Exp Brain Res 69:651–661. Medline

Maier A, Wilke M, Aura C, Zhu C, Ye FQ, Leopold DA (2008) Divergence of fMRI and neural signals in V1 during perceptual suppression in the awake monkey. Nat Neurosci 11:1193–1200. CrossRef Medline

Maier A, Aura CJ, Leopold DA (2011) Infragranular sources of sustained local field potential responses in macaque primary visual cortex. J Neurosci 31:1971–1980. CrossRef Medline

Mohler CW, Wurtz RH (1977) Role of striate cortex and superior colliculus in visual guidance of saccadic eye movements in monkeys. J Neurophysiol 40:74–94. Medline

Oostenveld R, Fries P, Maris E, Schoffelen JM (2011) FieldTrip: open source software for advanced analysis of MEG, EEG, and invasive electrophysiological data. Comput Intell Neurosci 2011:156869. CrossRef Medline

Poulet JF, Fernandez LM, Crochet S, Petersen CC (2012) Thalamic control of cortical states. Nat Neurosci 15:370–372. CrossRef Medline

Ray S, Maunsell JH (2011) Different origins of gamma rhythm and high-gamma activity in macaque visual cortex. PLoS Biol 9:e1000610. CrossRef Medline

Rodman HR, Sorenson KM, Shim AJ, Hexter DP (2001) Calbindin immunoreactivity in the geniculo-extrastriate system of the macaque: implications for heterogeneity in the koniocellular pathway and recovery from cortical damage. J Comp Neurol 431:168–181. CrossRef Medline

Roopun AK, Middleton SJ, Cunningham MO, Lebeau FE, Bibbig A, Whittington MA, Traub RD (2006) A beta2-frequency (20–30 Hz) oscillation in nonsynaptic networks of somatosensory cortex. Proc Natl Acad Sci U S A 103:15646–15650. CrossRef Medline

Roopun AK, Lebeau FE, Rammell J, Cunningham MO, Traub RD, Whittington MA (2010) Cholinergic neuromodulation controls directed tempo-

ral communication in neocortex in vitro. Front Neural Circuits 4:8. CrossRef Medline

Saalmann YB, Pinsk MA, Wang L, Li X, Kastner S (2012) The pulvinar regulates information transmission between cortical areas based on attention demands. Science 337:753–756. CrossRef Medline

Salazar RF, Dotson NM, Bressler SL, Gray CM (2012) Content-specific fronto-parietal synchronization during visual working memory. Science 338:1097–1100. CrossRef Medline

Schmid MC, Panagiotaropoulos T, Augath MA, Logothetis NK, Smirnakis SM (2009) Visually driven activation in macaque areas V2 and V3 without input from the primary visual cortex. PLoS One 4:e5527. CrossRef Medline

Schmid MC, Mrowka SW, Turchi J, Saunders RC, Wilke M, Peters AJ, Ye FQ, Leopold DA (2010) Blindsight depends on the lateral geniculate nucleus. Nature 466:373–377. CrossRef Medline

Schmid MC, Schmiedt JT, Peters AJ, Saunders RC, Maier A, Leopold DA (2013) Motion-sensitive responses in visual area v4 in the absence of primary visual cortex. J Neurosci 33:18740–18745. CrossRef Medline

Stepniewska I, Qi HX, Kaas JH (1999) Do superior colliculus projection zones in the inferior pulvinar project to MT in primates? Eur J Neurosci 11:469–480. CrossRef Medline

Steriade M (1993) Cellular substrates of brain rhythms. In: Electroencephalography: basic principles, clinical applications, and related fields, Ed 3

(Niedermeyer E, Lopes da Silva FH, eds), pp 27–62. Baltimore: Williams and Wilkins.

Sun W, Dan Y (2009) Layer-specific network oscillation and spatiotemporal receptive field in the visual cortex. Proc Natl Acad Sci U S A 106:17986–17991. CrossRef Medline

Tallon-Baudry C, Mandon S, Freiwald WA, Kreiter AK (2004) Oscillatory synchrony in the monkey temporal lobe correlates with performance in a visual short-term memory task. Cereb Cortex 14:713–720. CrossRef Medline

Taylor K, Mandon S, Freiwald WA, Kreiter AK (2005) Coherent oscillatory activity in monkey area v4 predicts successful allocation of attention. Cereb Cortex 15:1424–1437. Medline

Wilke M, Logothetis NK, Leopold DA (2006) Local field potential reflects perceptual suppression in monkey visual cortex. Proc Natl Acad Sci U S A 103:17507–17512. CrossRef Medline

Wróbel A, Ghazaryan A, Bekisz M, Bogdan W, Kamiñski J (2007) Two streams of attention-dependent beta activity in the striate recipient zone of cat's lateral posterior-pulvinar complex. J Neurosci 27:2230–2240. CrossRef Medline

Xing D, Yeh CI, Burns S, Shapley RM (2012) Laminar analysis of visually evoked activity in the primary visual cortex. Proc Natl Acad Sci U S A 109:13871–13876. CrossRef Medline